



Published in final edited form as:

Biochim Biophys Acta. 2008 January ; 1780(1): 41–50.

Water structure *in vitro* and within *Saccharomyces cerevisiae* yeast cells under conditions of heat shock

Jennifer L. Dashnau¹, Laura K. Conlin, Hillary C. M. Nelson, and Jane M. Vanderkooi*

Johnson Research Foundation, Department of Biochemistry and Biophysics, School of Medicine, University of Pennsylvania, Philadelphia, Pennsylvania 19104

Abstract

The OH stretch mode from water and organic hydroxyl groups have strong infrared absorption, the position of the band going to lower frequency with increased H-bonding. This band was used to study water in trehalose and glycerol solutions and in genetically modified yeast cells containing varying amounts of trehalose. Concentration-dependent changes in water structure induced by trehalose and glycerol in solution were detected, consistent with an increase of lower-energy H-bonds and interactions at the expense of higher-energy interactions. This result suggests that these molecules disrupt the water H-bond network in such a way as to strengthen molecule-water interactions while perturbing water-water interactions. The molecule-induced changes in the water H-bond network seen in solution do not translate to observable differences in yeast cells that are trehalose-deficient and trehalose-rich. Although comparison of yeast with low and high trehalose showed no observable effect on intracellular water structure, the structure of water in cells is different from that in bulk water. Cellular water exhibits a larger preference for lower-energy H-bonds or interactions over higher-energy interactions relative to that shown in bulk water. This effect is likely the result of the high concentration of biological molecules present in the cell. The ability of water to interact directly with polar groups on biological molecules may cause the preference seen for lower-energy interactions.

Keywords

infrared; heat shock; hydrogen bond; trehalose; glycerol; *Saccharomyces cerevisiae*

1. Introduction

Small protective molecules, such as trehalose and glycerol, are widely found in a number of organisms including bacteria, yeasts, plants and insects. These molecules, many of which contain a large number of hydroxyl groups, have been correlated with protection of organisms from dehydration, temperature or osmotic stress [1-4]. However, details behind how these molecules accomplish their protective function within an organism remain under debate. In solution, small hydroxylated compounds such as trehalose and glycerol are known to interact with water molecules in the immediate hydration layer and distort the structure of the water H-bond network [5-10]. However, the question remains: are these molecules also able to

* Corresponding author. Tel: 215 898-8783, e-mail address: vanderko@med.upenn.edu.

¹Present address: Recombinant Vaccine Technology and Engineering, Merck & Co., Inc., West Point, Pennsylvania 19486

Publisher's Disclaimer: This is a PDF file of an unedited manuscript that has been accepted for publication. As a service to our customers we are providing this early version of the manuscript. The manuscript will undergo copyediting, typesetting, and review of the resulting proof before it is published in its final citable form. Please note that during the production process errors may be discovered which could affect the content, and all legal disclaimers that apply to the journal pertain.

influence the structure of water in cells, and is the biological molecule-induced water structuring responsible for protection against environmental extremes?

The yeast, *Saccharomyces cerevisiae*, serves as a good model organism for the study of protective molecule effects *in vivo*. In yeast, environmental stress can activate three transcriptional control elements—heat shock elements (HSEs), stress-response elements (STREs), and AP-1-responsive elements (APEs)—depending on the source of the stress [11]. These transcriptional elements trigger associated transcription factors—heat shock transcription factor (HSFs), Msn2,4 transcription factor, and Gcn4/Yap transcription factors, respectively—that are responsible for expression of a number of protective molecules and proteins. While the functions of these stress-response pathways overlap, there is some distinction in the types of stresses that normally activate each pathway. For instance, the HSFs regulated by HSEs generally produce heat shock proteins (HSPs) and trehalose responsible for protection against moderate high temperature-induced stresses. However, under cold temperature-induced stress, the STRE/Msn-2,4 pathway may be responsible for production of these same molecules [12,13]. Meanwhile, osmotic-stress generally triggers glycerol production through the high-osmolarity mitogen-activated protein kinase (HOG MAPK) signal transduction through the STRE/Msn-2,4 pathway [14]. Finally, oxidative stress and exposure to heavy metals may induce protection through the APE/Gcn4/YAP pathway [11].

Regardless of the method of transcriptional regulation, “heat shock response” activates production of a class of molecular chaperones called heat shock proteins and the small disaccharide trehalose, which have been implicated in protecting yeast cells under moderate high- and low-temperature stress. Additionally, initial exposure to moderate temperature stress can confer protection against more extreme temperatures, osmotic conditions, and dehydration [15]. The synergistic role of heat shock proteins and trehalose in the protection of yeast has been studied by Singer and Lindquist [16]. In the heat shock response, trehalose is responsible for stabilizing proteins in native state conditions and reducing aggregation of partially unfolded proteins when HSPs are unavailable. The HSPs are responsible for binding denatured proteins, preventing aggregation, and promoting refolding. While the high levels of trehalose produced upon heat shock are beneficial during the period of time in which HSPs are not in abundance, these concentrations of trehalose can be detrimental to full HSP activity once HSP levels are sufficiently up-regulated. Other works have come to similar conclusions that while trehalose aids in the absence of HSPs, heat shock proteins are ultimately responsible and essential for recovery from cellular stress. For instance, mutation of the gene responsible for trehalose synthesis, trehalose-6-phosphate synthase (*tps1*), leads to cells lacking trehalose that exhibit stress-tolerance slightly reduced from the wild-type strain; this result indicates that trehalose is beneficial, but may not be necessary for survival under environmental extremes [17]. Mutation of the gene responsible for trehalose catabolism, neutral trehalase (*nth1*), results in cells with consistently high levels of intracellular trehalose following heat shock [18]. These cells exhibit lower thermo-tolerance despite high trehalose concentration, thus suggesting that these concentrations can be detrimental to cell survival through interference with other stress-tolerance mechanisms.

These studies have been useful in addressing the general role of trehalose in stress protection. However, the specific mechanism through which trehalose accomplishes its preliminary protection remains unknown. Some groups have assumed that trehalose is involved in stabilization of cell membranes during temperature-stress [19]. This assumption would be in line with water-replacement [20] or vitrification hypotheses [21]. In the ‘water replacement hypothesis’, under conditions of extreme dehydration, water molecules naturally found bound between polar head groups of membrane phospholipids are replaced by contact with solutes such as the disaccharide trehalose. By interacting with phospholipids, trehalose is believed to maintain spacing between the head groups and decreases van der Waals interactions between

hydrocarbon chains—thus preventing collapse of the membrane to the gel state which can lead to cell damage. The vitrification hypothesis suggests that carbohydrate molecules act in a more indirect manner by forming a high viscosity, glassy state surrounding biological molecules which prevents molecular mobility and thus limits water loss, the ability of the solution to crystallize, and the propensity of biological molecules to precipitate or aggregate. Meanwhile, other groups suggest trehalose stabilizes proteins by raising the free energy of the denatured state relative to the native state [13]. This suggestion would correspond to the preferential exclusion model of protein stabilization [22].

Although a number of experimental and theoretical studies have addressed the effect of trehalose and glycerol on water structure and dynamics in solution, few studies have attempted to examine the effect of these compounds on water within cells. A search of literature published to date reveals only three articles that investigate the influence of trehalose or glycerol on intracellular water structure and dynamics; these articles employ ^1H NMR to determine the effect of trehalose concentration on intracellular water dynamics [23-25]. However, NMR is not the only spectroscopic technique that can be used for such investigations. While NMR can be used to study water dynamics, infrared spectroscopy can be used to study water structure in samples.

Infrared spectroscopy has been used previously in the study of whole cell systems mainly to identify cell strains or particular cellular components [26-30]. Infrared spectroscopy is a technique well suited for the study of water structure since changes in the OH stretch region of the spectra are indicative of changes in the local environment surrounding OH vibrational oscillators, so it is surprising that it has not yet been used to study intracellular water structure. However, the lack of IR intracellular water studies is most likely due to difficulties in preparing suitable samples. Two difficulties are involved in sample preparation. First, in order to examine intracellular water structure, the majority of extracellular water must be removed from the sample to prevent interference from this water component. However, in removing extracellular water from a sample, an osmotic imbalance is created and cells may become dehydrated. Second, the intracellular water must yield an infrared absorbance signal in the OH stretch region that is on-scale in order for proper interpretation of spectral changes. Unfortunately, water is a very good absorber of infrared energy so samples prepared for IR must be exceedingly thin—thinner than width of most cells.

In order to circumvent the difficulties associated with IR described above, we have developed an experimental procedure that addresses these limitations. In this work, Fourier-transform infrared spectroscopy is used to investigate the interaction of trehalose and glycerol with water *in vitro* and *in vivo*. The yeast *Saccharomyces cerevisiae* was selected as a model system due to its cellular properties. The presence of a rigid cell wall protects the cell from damage that may result from the removal of extracellular water, while allowing for efficient removal of extracellular water by filtration over a membrane. This process is gentler than other methods used to remove extracellular water, such as lyophilization. Also, cultures of this organism can easily be grown in liquid media containing a large amount of D_2O . The presence of D_2O reduces the IR absorption of the OH stretch to a level that is on-scale, thus facilitating analysis of results. Finally, yeast can be genetically manipulated to express varying levels of trehalose, thus making examination of small molecule effects on intracellular water structure possible. The results of the whole-cell IR experiments have been compared with temperature-dependent shifts in the OH stretch region of the IR spectra of trehalose and glycerol over a range of concentrations in solution; these data have been used to determine the effect these molecules have on the H-bonding network of water.

2. Experimental

2.1 Yeast strains and media

All yeast strains were derived from the *S. cerevisiae* W303-1A strain Y699 (*MATa ade2-1 trp1-1 can1-100 leu2,3-112 his3-11,15 ura3-1*). Gene knockouts of *NTH1* and *TPS1* were performed using drug-resistant gene disruption cassettes, as previously described [31,32]. Briefly, primers were used to amplify a disruption construct consisting of the resistance gene flanked with homologous genomic sequence. For the *nth1Δ* strain (YHN432), primers LC9 (ATAAACAAAAAAGAAAAATTAACAAAAAAATCAGTAGAGCATAGGCCACT AGTGGATCTG) and LC10 (TACCTGGAGTATATATATATATATATATATTATCTCAACAGCTGAAGCTTCG TACGC) were used, and primers LC1 (AACTAGGTACTCACATACAGACTTATTAAGACATAGAACTGCATAGGCCACTA GTGGATCTG) and LC2 (GGACCAGGAATAGACGATCGTCTCATTTGCATCGGGTTCACAGCTGAAGCTTCG TACGC) were used for the *tps1Δ* strain (YHN429), to amplify the *hphMX4* cassette from the plasmid pAG32 [33]. The amplified cassettes were then transformed into the various yeast strains, and proper integration of the reporter was verified by PCR. Deletion of *tps1* and *nth1* genes produces yeast cells that are incapable of synthesizing and breaking down trehalose within the cell. As a result, YHN429 (*tps1Δ*) fails to accumulate trehalose during normal growth or heat shock. Alternatively, YHN432 (*nth1Δ*) accumulates and retains trehalose in high concentration during normal growth and heat shock.

Because *tps1Δ* strains can not grow with glucose as a carbon source [34-36], all strains were grown in synthetic complete media (Sc) with 80% D₂O and 2% galactose as a carbon source. Amino acids were supplemented as necessary [37]. Aminoglycosides were included at concentrations of 200 μg/ml Hygromycin B (Roche). For all experiments, cells were grown at 30°C to mid-logarithmic phase (OD₆₀₀ of 0.3 to 0.5). For heat-shocked samples, cells were transferred to a heated water bath at 37°C for 90 minutes.

2.2. Cell hydration

Yeast cells were harvested by pelleting. The cells were then resuspended and washed twice in 1 mL D₂O to remove traces of media from the cells. The cells were then suspended in 400 ul D₂O and filtered for two minutes by centrifugation over a Montage-PCR filter (Millipore, Bedford, MA). Another 400 ul of D₂O was added to the cells and the sample was centrifuged for an additional 10 minutes to remove residual extracellular water. Filters containing the cell pellets were placed in a vacuum desiccator containing calcium sulfate for 48 hours in order to allow for the loss of intracellular water. The weight of the pellet before and after desiccation was used to determine approximate mass percentage of water within the cells.

2.3. Trehalose and glycerol assays

Trehalose and glycerol were isolated from yeast cells according to the following procedure. Yeast cells were harvested by pelleting and residual extracellular water was removed by centrifuging samples over a Montage PCR filter (Millipore, Bedford, MA). Cells were washed twice in water and the cell pellets were resuspended in a volume of lysis buffer—containing 50 mM HEPES, pH 7.5, 150 mM NaCl, 1 mM EDTA, 1% Triton X-100, 0.1% sodium deoxycholate, and 0.1% SDS—equal to twice the measured weight. For example, if the weight of the pellet totaled 20 mg, then 40 ul of water was added. The cells were placed in a boiling water bath for 5 minutes. Glass beads, 425-600 microns (Sigma, St. Louis, MO) were then added to the cells and the solution was vortexed for 5 minutes at high setting. The cells were spun down and the supernatant was removed for use in enzymatic analyses.

Glycerol concentration was assayed utilizing Free Glycerol Reagent kit (Sigma, St. Louis, MO). All samples were assayed according to directions outlined in the accompanying technical bulletin. Briefly, 2.5 μ l of water, glycerol standard (0.26 mg/ml), or sample was added to a cuvette containing 200 μ l of reconstituted, room-temperature free glycerol reagent. The blank, standard, and samples were incubated for 15 minutes at room temperature to allow the conversion of glycerol to a visible dye through a series of coupled enzyme reactions involving glycerol kinase, glycerol phosphate oxidase, and peroxidase present within the free glycerol reagent. Absorbance of the final product, a quinoneimine dye, was measured at 540 nm on a visible spectrometer (Amersham Biosciences) and was directly proportional to the concentration of glycerol in the sample [38,39].

Trehalose concentration was assayed in a two-part procedure. First, trehalose was enzymatically converted to glucose through reaction with trehalase (Sigma, St. Louis, MO) according to the testing procedure provided in the product information [40]. For each standard or sample to be tested, assay reagent was mixed by adding 20 μ l of trehalase enzyme solution (0.1 to 0.3 units/ml) to 60 μ l of 135 mM citric acid buffer, pH 5.7. Following equilibration of the assay reagent to 37°C in a heated water bath, 20 μ l of water, 140 mM trehalose standard in citric acid buffer, or sample was added separately to the assay reagent. The solutions were equilibrated and incubated in a 37°C water bath for eight hours, following which 100 μ l of 500 mM Tris buffer, pH 7.5 was added to each reaction.

The second part of the trehalose concentration assay involved determining glucose concentration using the Glucose (HK) Assay Kit (Sigma, St. Louis, MO) [41-43]. For each sample in the trehalase reaction described above, 6.7 μ l of sample was added to 200 μ l of glucose assay reagent. In order to determine the amount of glucose arising from trehalose, the naturally occurring glucose present in the cell was also determined. For these samples, 6.7 μ l of sample from cells was reacted with 200 μ l glucose assay reagent. Sample blank were also required; 6.7 μ l of sample was mixed with 200 μ l water. The blank, standard, and samples were incubated for 15 minutes at room temperature to allow the conversion of glucose to 6-phosphogluconate through coupled enzyme reactions involving hexokinase and glucose-6-phosphate dehydrogenase present within the reagent. Absorbance of NADH, a by-product produced from these reactions, was measured at 340 nm on a visible spectrometer (Amersham Biosciences) and was directly proportional to the concentration of glucose in the sample.

2.4. Infrared sample preparation

Yeast samples were prepared for analysis as follows. A 50 mL culture of exponential phase yeast cells or exponential phase heat-shocked yeast cells grown in media containing approximately 80% D₂O was centrifuged for 5 minutes on a table top centrifuge to remove excess media. The cells were then resuspended and washed twice in 1 mL D₂O to remove traces of media from the cells. The cells were then suspended in 400 μ l D₂O, and filtered for two minutes by centrifugation over a Montage-PCR filter (Millipore, Bedford, MA). Another 400 μ l of D₂O was added to the cells and the sample was centrifuged for an additional 10 minutes to remove extracellular water. The yeast pellet was scraped from the filter and placed between two CaF₂ windows. Pressure was applied manually to the windows to spread the cells into a thin layer across the entire window and to remove any air bubbles or remaining moisture from the sample.

Trehalose, glycerol and water controls were also prepared for infrared analysis. The deuterated water control was prepared to 80:20 D₂O/H₂O (v/v) using distilled, deionized water and 99 atom % D deuterium oxide (Sigma, St. Louis, MO). Glycerol mixtures were prepared by dilution of an initial 80:20 glycerol-D₃/glycerol (w/w) solution with the appropriate amount of 80:20 D₂O/H₂O (v/v) to yield glycerol concentrations of 2 M, 1 M, 500 mM, 250 mM, and 125 mM. Glycerol-D₃ and glycerol were provided by Cambridge Isotope Labs (Cambridge,

MA) and Sigma (St. Louis, MO), respectively. Trehalose controls were made as follows. Solid α,α -trehalose (Sigma, St. Louis, MO) was lyophilized following dissolution in an excess volume of 80:20 D₂O/H₂O (v/v). The resulting solid was then resuspended in 80:20 D₂O/H₂O (v/v) to 1 M concentration and dilutions in 80:20 D₂O/H₂O (v/v) were prepared to yield final concentrations of 500 mM, 250 mM, 125 mM and 62.5 mM. Approximately 7 μ l of each sample was placed between two CaF₂ windows for measurement.

2.5. Infrared spectra and analysis

Infrared spectra were obtained with a Bruker IFS 66 Fourier transform IR spectrophotometer (Bruker, Brookline, MA). The sample compartment was purged with nitrogen to reduce the contribution from carbon dioxide and water vapor. The signal was monitored using an HgCdTe (MCT) detector. The sample temperature was lowered at a rate of 3°C/min from 30°C to -14°C by a Neslab RTE 740 water bath (Thermo Electron Corp., Waltham, MA) and was monitored using a Fisherbrand Traceable Total-Range digital thermometer (Fisher Scientific International Inc., Hampton, NH). All spectra were taken in transmission mode with an aperture of 2.0 mm and a spectral resolution of 2 cm⁻¹. Spectra were processed with atmospheric correction, Savitsky-Golay smoothing, baseline correction and conversion to absorbance in OPUS v.5.0 (Bruker) prior to area analysis. Spectra were normalized in the 3000 to 4000 cm⁻¹ range to facilitate comparison of OH stretch data or in the 1150 to 1350 cm⁻¹ range for DOD bend data.

OPUS v.5.0 (Bruker) was used to integrate the area under the OH stretch bounded by 3100 cm⁻¹ and 3700 cm⁻¹ with a linear baseline between these points. Following a procedure similar to that of Smith, et.al., the region was divided into two area contributions of low (A₁) and high (A₂) energy using 3450 cm⁻¹ as the line of separation [44]. These areas were used to determine the change in free energy, ΔG° , associated with the transition from high to low energy populations according to the formula: $\Delta G^{\circ} = -RT(\ln(A_1/A_2))$ [45]. The change in free energy of this transition as a function of temperature was plotted in Excel (Microsoft).

3. Results

3.1. IR spectra of water and trehalose

The OH group is a strong absorber of infrared light. In Figure 1, the spectrum of 1 M trehalose in 95% D₂O and 5% H₂O is shown. The off-scale peak represents the O-D absorption. The band at 2950 cm⁻¹ includes contributions from CH and CH₂ stretching modes arising from the sugar. Peaks below 1500 cm⁻¹ include contributions from HOH, HOD and DOD bending modes as well as contributions from the sugar [46]. The absorption band between 3200 and 3600 cm⁻¹ is what concerns us. This is the OH stretching band. As can be seen in the figure, as temperature increases, this band goes to higher frequency.

3.2. Analysis of the OH absorption as a function of temperature

The OH stretching band of solutions of trehalose and glycerol were analyzed as described in Methods and values of $\Delta G_{h \rightarrow l}^{\circ}$ were plotted as a function of temperature (Figure 2). Across all concentrations and temperatures studied, the free energy of transition was favorable—as indicated by the negative $\Delta G_{h \rightarrow l}^{\circ}$ values. As temperature was lowered, the $\Delta G_{h \rightarrow l}^{\circ}$ values became more negative; each condition had a decrease in $\Delta G_{h \rightarrow l}^{\circ}$ of nearly 200 cal mol⁻¹ over the temperature range studied (303 K to about 263 K). This result indicates that as temperature is lowered, the environment surrounding OH oscillators favors lower-energy interactions. In the case of H-bonds formed by the OH oscillator and atoms in the local environment, the shift to lower-energy interactions would suggest a slight strengthening of the H-bond through a decrease in H-bond distance, linearization of H-bond angle, or some combination of the two.

Concentration of solute had a similar effect on $\Delta G_{h \rightarrow l}^0$. For both trehalose and glycerol, increase in concentration lowered the free energy of transition at any given temperature. In the concentration range studied, the decrease in $\Delta G_{h \rightarrow l}^0$ was as large as 50 cal mol^{-1} for the highest concentrations. The effect on the free energy of transition appears to be related to the hydroxyl content of the two solutes. A 2 M concentration of glycerol was needed to approach the effect obtained by 1M trehalose; glycerol, with its three hydroxyl groups, must be about twice as concentrated as trehalose, which contains eight hydroxyl groups.

Trehalose and glycerol can also be found naturally in certain organisms. In yeast, these solutes are involved in various stress response pathways involving protection from thermal and osmotic extremes [1,4,12-14,33,47]. In order to examine the effects of trehalose and glycerol on water structure inside the cell, trehalose-deficient (YHN429, *tps1Δ*) and trehalose-rich (YHN432, *nth1Δ*) yeast strains were used. Enzymatic assays of trehalose and glycerol concentration revealed that while the levels of glycerol remain fairly constant at 25 to 35 mM under constitutive and heat-shock conditions in both strains, trehalose levels vary more widely. Trehalose-deficient yeast (YHN429, *tps1Δ*) does not show appreciable levels of trehalose under constitutive or heat shock conditions, while trehalose-rich yeast (YHN432, *nth1Δ*) contain approximately 45 mM trehalose and 135 mM trehalose under constitutive and heat-shock conditions, respectively. Therefore, trehalose appears to be the solute accumulated under these experimental conditions.

The infrared OH stretch mode in yeast was analyzed to determine the effect of trehalose on intracellular water structure (Figure 3). As in the trehalose controls, a decrease in temperature caused a decrease in the free energy of transition with a magnitude approximately 200 cal mol^{-1} over the temperature range studied. Additionally, the value of $\Delta G_{h \rightarrow l}^0$ of the yeast strains is more negative than that of the water control at all temperatures. However, there is no visible difference between yeast strains that can be ascribed to trehalose concentration—despite the presence of what should be a detectable concentration of trehalose in the heat-shocked, trehalose-rich *nth1Δ* strain. A primary problem with analysis of the yeast strains is that the error associated with the replicates of each strain is 5 to 10 times larger than that of the *in vitro* trehalose controls. The higher error may obscure subtle differences between the strains due to trehalose content since the magnitude of the error is larger than the overall expected change in the value of $\Delta G_{h \rightarrow l}^0$ that is due to trehalose concentration.

3.3 Effect of deuteration on OH stretch

The larger variation between batches of yeast may be unavoidable, as differences in deuteration level and cell contents between batches are likely the cause. To illustrate this, Figure 4 shows that the level of deuteration present in a sample impacts $\Delta G_{h \rightarrow l}^0$. As explained earlier, high concentrations of D relative to H are used to isolate OH oscillators and reduce resonance energy transfer between other OH groups. This method allows for the use of the OH stretch mode as an indicator of changes in the local environment surrounding an OH oscillator. In our analysis method, a higher D content leads to more negative, or favorable, $\Delta G_{h \rightarrow l}^0$ in the entire temperature range studied. However, the differences between samples with varying D content become even more pronounced as temperature is lowered; there is a greater difference in $\Delta G_{h \rightarrow l}^0$ between samples at lower temperature than at higher temperature. This result may be caused by the inherent nature of the infrared OH stretch mode. The integrated intensity of the OH stretch increases as H-bonds or interactions are enhanced due to temperature, molecular arrangement, or other factors [48,49]. Since lower-energy bonds increase as temperature decreases, this difference in intensity would be more pronounced at these temperatures. The larger differences at lower temperature may explain the variation between yeast batches. The error between yeast samples at higher temperature is less than that at lower temperature.

The level of deuteration present in a sample can be monitored by the relative ratio of DOD:HOD:HOH bending modes since these modes represent contributions from water vibrations alone. As can be seen in Figure 5 for the water controls, as H content is increased and D content decreased, the intensity of the HOD and HOH modes relative to the normalized DOD mode increase. The relative intensity of the HOD and HOH to DOD modes for replicates of a single yeast strain and condition (YHN432, *nth1Δ*, constitutive/non heat-shocked conditions) show that the D content of the yeast cells is much higher than the media in which the cells were grown. The D content exceeds 90%. Additionally, there is variation among the replicates. However, deuteration level alone is not completely sufficient to explain the degree of variation between yeast replications. Cellular components may also influence the free energy transition. As is shown in Figure 4, numerous yeast modes overlap the HOD and HOH modes of the spectra. While changes in deuteration may influence the intensity of these modes, the intensity may also be influenced by changes in the identity or level of cellular components between batches as well.

4. Discussion

4.1 Trehalose and glycerol affect the water network in a concentration-dependent manner

Trehalose and glycerol in solution influence the infrared OH stretch mode of water in a concentration-dependent manner. An increase in concentration of these solutes leads to a decrease in $\Delta G_{h \rightarrow i}^0$, which indicates that lower-energy H-bonds or interactions with OH oscillators become relatively more favorable than their higher-energy counterparts. Conceptually, this result can be explained in two ways. Under the first interpretation, the solute can interact with water in a manner which increases the strength of interactions between water molecules in the neighboring hydration shell. Hydrogen bonds between water molecules in the surrounding hydration layer are strengthened—suggesting that the bonds experience a decrease in H-bond length, linearization of H-bond angle, or some combination of changes on geometric orientation. In the alternative explanation, water-water H-bonds in the hydration layer surrounding the solute molecule are not strengthened. Rather, the solute interacts directly with surrounding water molecules. This scenario means that while hydration waters may experience a greater degree of distortion between water-water interactions, the interaction between solute atoms and water would be strengthened. For the case of H-bonds between solute hydroxyl groups and water, strengthening of the H-bond could be ascribed to decrease in bond length, linearization of bond angle, or a combination of these effects.

The second explanation is supported by a number of experimental and theoretical studies for trehalose and glycerol. Trehalose, and its interaction with water, has been studied extensively using inelastic neutron scattering and optical spectroscopy techniques [5,6,9]. These studies indicate that trehalose has a great destructuring effect on the H-bond network of surrounding water molecules that is due in part to its unusually large hydration volume that forms as a result of water H-bonding to trehalose hydroxyl groups. Increasing the concentration of trehalose exacerbates these effects as the relative percentage of bound water molecules to free water molecules increases, where ‘bound’ and ‘free’ refer to water molecules influenced by solute interactions and those independent of solute interaction, respectively.

Additionally, molecular dynamics simulations support the perturbation of water structure by trehalose [10]. The stereochemical topology and solution conformation of trehalose allow this solute to interact with surrounding water molecules. Bidentate H-bonds involving water and trehalose hydroxyl groups were found extensively; water molecules were found bridging adjacent hydroxyl groups and bridging hydroxyl groups on separate glucose-monomers of the trehalose molecule. The structuring of water by trehalose affected not only the immediate hydration shell, but extended into solution up to three hydration layers out.

Similar perturbation of water can be seen in glycerol solutions [7]. Molecular dynamics simulations and infrared spectroscopy of glycerol solutions across a large range of concentrations showed that lower-energy interactions between glycerol and water become more favorable with increasing glycerol concentration. The infrared OH stretch mode shifts to lower wavenumber with increasing glycerol concentration. Simulations of solution showed that the majority of this shift arose from the interactions between glycerol hydroxyl groups and water, rather than the interaction between water molecules. These results suggest that H-bonds formed between glycerol and water increase slightly in strength, possibly through changes in orientation of the atoms involved in the H-bond.

4.2. The intracellular water network appears unaffected by trehalose concentration

Although the concentration of trehalose, a known cryoprotectant, varies within yeast cells, the behavior of the OH stretch within the cell remains unaffected. There are a number of explanations for this result. The first explanation is that the concentration of trehalose in the trehalose-rich yeast strains is high enough to observe an effect relative to the trehalose-deficient strains, but the batch-to-batch variability obscures the results. Alternatively, trehalose may have an effect on the intracellular water network, but the concentration of trehalose present in these cells may not be high enough to induce an effect. Since the trehalose concentrations in the trehalose-rich (YHN432, *nth1Δ*) strains are artificially high relative to normal yeast cells, this result suggests that trehalose concentration in normal, living yeast cells does not become high enough to influence the structure of the water network. Finally, trehalose, under physiological intracellular concentrations, may not influence the water network in the cell; the role of trehalose may not be in altering water structure, rather in interacting with and stabilizing biomolecules.

It is already apparent from Figures 1 and 2 that the batch-to-batch variability is larger than the shift in $\Delta G_{h \rightarrow l}^0$ that would be expected for the amount of trehalose within the cells. Trehalose reaches approximately 150 mM (4% of dry cell weight) in the strain with the highest content. This difference is visible in the *in vitro* controls as the controls exhibit a smaller degree of error. However, the magnitude of the difference is most likely not enough to overcome the degree of error associated with the *in vivo* sample measurements. Although efforts were undertaken to ensure deuteration and culture-to-culture differences were minimized, the error associated with biological samples was nearly 10 times larger than that associated with non-biological controls.

However, it is also possible that the trehalose content may not be high enough to visibly alter intracellular water structure under the current method. Previous studies by Sano, *et al* used thermogravimetry and ^1H NMR to study water dynamics in commercial compressed bakers' yeast containing different amounts of trehalose and levels of rehydration [24]. Intracellular water can be divided into water molecules strongly associated with biological molecules (15% of intracellular water) and those that are relatively free, or outside of the immediate biological molecule hydration layer (85% of cellular water) [24]. In their study, trehalose content was found to replace bound water molecules when in concentrations greater than 2-3% of the dry cell weight. Additionally, in cases of extreme dehydration, the presence of a large concentration of trehalose allowed more bound water to be retained [23]. However, in our study, the yeast cells were purposefully not as dehydrated as those in the Sano study in order to investigate trehalose-induced water structure under normal hydration conditions. Therefore, the effect of trehalose on bound water will not be observed since the contribution of free water to the OH stretch will likely be much smaller than the contribution of bound water by a ratio of over 6:1. However, Sano, *et al* observed in more hydrated samples that at concentrations above 3-4% of the dry cell weight, trehalose was shown to slow the relaxation of intracellular water [24]. Longer water relaxation times are indicative of restriction of water movement, presumably

through increased strength of H-bonding between trehalose and water molecules. Since the highest trehalose content of cells in our study was approximately 4%, the resulting effect of trehalose on changes in water structure should be within the concentration range that effects start to be seen. Therefore, it remains likely that in trehalose-rich cells a change in water, although minimal, exists but is obscured by high variation in measurements presented by the technique employed.

4.3. The water network in yeast differs from bulk water

Although the effect of trehalose on intracellular water structure remains questionable, visible difference between intracellular water and bulk water are evident. These differences appear irrespective of trehalose or glycerol concentration. As shown in Figure 2, the $\Delta G_{h \rightarrow l}^{\circ}$ values for all yeast strains are lower than that of the bulk control. This result suggests that intracellular water network interactions are slightly more favorable than the interactions found in bulk water. To interpret these results further, one can look to model system and whole-cell NMR studies.

Reverse micelles, or microemulsions consisting of water pools surrounded by amphiphilic membranes in nonpolar solvent, are often used as a model system for the study of water and molecules in confined conditions that mimic the environment of the cell. Water structure in reverse micelles differs from that of bulk water as exhibit by a shift in $\Delta G_{h \rightarrow l}^{\circ}$ [45]. As the amount of water in these structures is decreased, the effect of the surrounding membrane on water structure is more evident; that is, the $\Delta G_{h \rightarrow l}^{\circ}$ becomes more positive, or unfavorable, relative to bulk water conditions. This result is in contrast to what is observed for the water network in yeast cells. The difference in the direction of the shift is likely attributed to the simplified nature of the reverse micelle model system compared to intracellular conditions. Water in reverse micelle systems is influenced mainly by the charged head groups and counter ions of the amphiphilic membrane. As has been shown previously, charged groups induce drastic changes on surrounding water structure [50]. Ions distort surrounding water structure, causing higher-energy water-water interactions to increase at expense of lower-energy interactions—hence why the reverse micelle data show a more positive $\Delta G_{h \rightarrow l}^{\circ}$ relative to bulk water.

However, inside of the cell, water molecules are likely to encounter a number of different types of molecules and interactions due to the diversity of cell contents. While charged groups are undoubtedly present, hydrophobic and polar interactions can also be found. Polar interactions, specifically, are likely to contribute to changes in water structure as they may be able to form H-bonds directly with surrounding water molecules. As is the case with trehalose *in vitro*, the polar groups of biological molecules are likely able to H-bond with water molecules and thus induce stronger biomolecule-water interactions. These strengthened interactions would translate to the negative shift of $\Delta G_{h \rightarrow l}^{\circ}$ seen for yeast relative to bulk water.

NMR studies using water proton spin-lattice relaxation times in whole-cells support this idea [23,51,52]. As shown by Raaphorst et al, the direct effect of ions on influencing surrounding intracellular water is small, rather ions influence water molecules indirectly by altering biomolecule hydration [52]. Since ions alone show little effect on intracellular water in the absence of biomolecules, the differences between the reverse micelle model system and yeast are not as alarming. Additionally, self-diffusion constants and NMR relaxation times have shown for hen egg white and yolk, that much of the decrease in intracellular water mobility is due to hydration of biomolecules [51]. The involvement of biomolecule hydration in the reduction in intracellular water relaxation times likely stems from macromolecular crowding which mechanically hinders water diffusion or from direct physical interaction of biomolecules with water, as would be expected if biomolecules formed H-bonds with surrounding hydration waters. The decrease in $\Delta G_{h \rightarrow l}^{\circ}$ in yeast relative to bulk water supports the latter explanation.

5. Conclusion

In this study IR spectroscopy was used to examine water in yeast cells. Cellular water exhibits a larger preference for lower-energy H-bonds or interactions over higher-energy interactions relative to that shown in bulk water. This effect is likely the result of the high concentration of biological molecules present in the cell. The ability of water to interact directly with polar groups on biological molecules may cause the preference seen for lower-energy interactions. Concentration-dependent changes in water structure induced by trehalose and glycerol are detectable through IR spectroscopy. As concentration of these molecules in solution is increased, water structure is perturbed—resulting in an increase of lower-energy H-bonds or interactions at the expense of higher-energy interactions. This result suggests that these molecules disrupt the water H-bond network in such a way as to strengthen molecule-water interactions while perturbing water-water interactions. However, the molecule-induced changes in the water H-bond network seen in solution do not translate to differences within the error of measurement in yeast cells that are trehalose-deficient and trehalose-rich.

Acknowledgements

This project was supported by the National Research Initiative of the USDA Cooperative State Research, Education and Extension Service, grant number 2005-35503-16151. LKC and HCMN were supported by NIH grant number GM44086.

References

1. Carvalheiro F, Roseiro JC, Girio FM. Interactive effects of sodium chloride and heat shock on trehalose accumulation and glycerol production. *Food Microbiol* 1999;16:543–550.
2. Gadd GM, Chalmers K, Reed RH. The role of trehalose in dehydration resistance of *Saccharomyces cerevisiae*. *FEMS Microbiol Lett* 1987;48:249–254.
3. Hino A, Mihara K, Nakashima K, Takano H. Trehalose levels and survival ratio of freeze-tolerant versus freeze-sensitive yeasts. *Appl Environ Microbiol* 1990;56:1386–1391. [PubMed: 2339891]
4. Izawa S, Sato M, Yokoigawa K, Inoue Y. Intracellular glycerol influences resistance to freeze stress in *Saccharomyces cerevisiae*: analysis of a quadruple mutant in glycerol dehydrogenase genes and glycerol-enriched cells. *Appl Microbiol Biotechnol* 2004;66:108–114. [PubMed: 15127164]
5. Branca C, Magazu S, Maisano G, Bennington SM, Fak B. Vibrational studies on disaccharide/H₂O systems by inelastic neutron scattering, Raman, and IR spectroscopy. *J Phys Chem B* 2003;107:1444–1451.
6. Branca C, Magazu S, Maisano G, Migliardo P. α,α -Trehalose-water solutions. 3. Vibrational dynamics studies by inelastic light scattering. *J Phys Chem B* 1999;103:1347–1353.
7. Dashnau JL, Nucci NV, Sharp KA, Vanderkooi JM. Hydrogen bonding and the cryoprotective properties of glycerol/water mixtures. *J Phys Chem B* 2006;110:13670–13677. [PubMed: 16821896]
8. Dashnau JL, Sharp KA, Vanderkooi JM. Carbohydrate intramolecular hydrogen bonding cooperativity and its effect on water structure. *J Phys Chem B* 2005;109:24152–24159. [PubMed: 16375407]
9. Lerbret A, Bordat P, Affouard F, Guinet Y, Hedoux A, Paccou L, Prevost D, Descamps M. Influence of homologous disaccharides on the hydrogen-bond network of water: complementary Raman scattering experiments and molecular dynamics simulations. *Carbohydr Res* 2005;340:881–887.
10. Liu Q, Schmidt RK, Teo B, Karplus PA, Brady JW. Molecular dynamics studies of the hydration of α,α -trehalose. *J Am Chem Soc* 1997;119:7851–7862.
11. Ruis H, Schueller C. Stress signaling in yeast. *Bioessays* 1995;17:959–965. [PubMed: 8526890]
12. Hayashi M, Maeda T. Activation of the HOG pathway upon cold stress in *Saccharomyces cerevisiae*. *J Biochem* 2006;139:797–803. [PubMed: 16672281]
13. Kandror O, Bretschneider N, Kreydin E, Cavalieri D, Goldberg AL. Yeast adapt to near-freezing temperatures by STRE/Msn2,4-dependent induction of trehalose synthesis and certain molecular chaperones. *Mol Cell* 2004;13:771–781. [PubMed: 15053871]
14. Wojda I, Alonso-Monge R, Bebelman J-P, Mager WH, Siderius M. Response to high osmotic conditions and elevated temperature in *Saccharomyces cerevisiae* is controlled by intracellular

glycerol and involves coordination activity of MAP kinase pathways. *Microbiol* 2003;149:1193–1204.

15. Parsell, DA.; Lindquist, S. The Biology of Heat Shock Proteins and Molecular Chaperones. Morimoto, RI.; Tissieres, A.; Georgopoulos, C., editors. Cold Spring Harbor Laboratory Press; Cold Spring Harbor, NY: 1994. p. 457-494.
16. Singer MA, Lindquist S. Multiple effects of trehalose on protein folding in vitro and in vivo. *Mol Cell* 1998;1:639–648. [PubMed: 9660948]
17. Ratnakumar S, Tunnaclyffe A. Intracellular trehalose is neither necessary nor sufficient for desiccation tolerance in yeast. *FEMS Yeast Res* 2006;6:902–913. [PubMed: 16911512]
18. Nwaka S, Kopp M, Burgert M, Deuchler I, Kienle I, Holzer H. Is thermotolerance of yeast dependent on trehalose accumulation? *FEBS Lett* 1994;344:225–228. [PubMed: 8187889]
19. Hochachka, P.; Somero, G. Biochemical Adaptations Mechanisms and Processes in Physiological Evolution. Oxford University Press; New York: 2002.
20. Crowe JH, Crowe LM, Chapman D. Preservation of membranes in anhydrobiotic organisms: the role of trehalose. *Science* 1984;223:701–703. [PubMed: 17841031]
21. Koster K, Webb WS, Bryant G, Lynch DV. Interactions between soluble sugars and POPC during dehydration: vitrification of sugars alters the phase behavior of the phospholipid. *Biochim Biophys Acta* 1994;1193:143–150. [PubMed: 8038184]
22. Shimizu S, Smith DJ. Preferential hydration and the exclusion of cosolvents from protein surfaces. *J Chem Phys* 2004;121:1148–1154. [PubMed: 15260652]
23. Sakurai M, Kawai H, Inoue Y, Hino A, Kobayashi S. Effects of trehalose on the water structure in yeast cells as studied by *in vivo* 1H NMR spectroscopy. *Bull Chem Soc Jpn* 1995;68:3621–3627.
24. Sano F, Asakawa N, Inoue Y, Sakurai M. A dual role for intracellular trehalose in the resistance of yeast cells to water stress. *Cryobiology* 1999;39:80–87. [PubMed: 10458903]
25. Turov VV, Gun'ko VM, Bogatyrev VM, Zarko VI, Gorbik SP, Pakhlov EM, Leboda R, Shulga OV, Chuiko AA. Structured water in partially dehydrated yeast cells and at partially hydrophobized fumed silica surface. *J Colloid and Interface Sci* 2005;283:329–343. [PubMed: 15721902]
26. Hopkinson JH, Moustou C, Reynolds N, Newbery JE. Applications of attenuated total reflection in the infrared analysis of carbohydrates and biological whole cell samples in aqueous solution. *Analyst* 1987;112:501–505. [PubMed: 3592248]
27. Kummerle M, Scherer S, Seiler H. Rapid and reliable identification of food-borne yeasts by Fourier-transform infrared spectroscopy. *Appl Environ Microbiol* 1998;64:2207–2214. [PubMed: 9603836]
28. Levine S, Stevenson HJR, Bordner RH. Identification of glycogen in whole bacterial cells by infrared spectrophotometry. *Science* 1953;118:141–142. [PubMed: 13076218]
29. Ngo-Thi NA, Kirschner C, Naumann D. Characterization and identification of microorganisms by FT-IR microspectrometry. *J Mol Structure* 2003;661-662:371–380.
30. Schultz C, Naumann D. In vivo study of the state of order of the membranes of Gram-negative bacteria by Fourier-transform infrared spectroscopy (FT-IR). *FEBS* 1991;294:43–46.
31. Goldstein AL, McCusker JH. Three new dominant drug resistance cassettes for gene disruption in *Saccharomyces cerevisiae*. *Yeast* 1999;15:1541–1553. [PubMed: 10514571]
32. Guldener U, Heck S, Fielder T, Beinhauer J, Hegemann JH. A new efficient gene disruption cassette for repeated use in budding yeast. *Nucl Acids Res* 1996;24:2519–2524. [PubMed: 8692690]
33. Conlin LK, Nelson HCM. The natural osmolyte trehalose is a positive regulator of the heat-induced activity of yeast heat shock transcription factor. *Mol and Cell Biol* 2007;27:1505–1515. [PubMed: 17145780]
34. Bell W, Klaassen P, Ohnacker M, Boller T, Herweijer M, Schoppink P, Van der Zee P, Wiemken A. Characterization of the 56-kDa subunit of yeast trehalose-6-phosphate synthase and cloning of its gene reveal its identity with the product of CIF1, a regulator of carbon catabolite inactivation. *Eur J Biochem* 1992;209:951–9. [PubMed: 1425702]
35. Van Aelst L, Hohmann S, Bulaya B, de Koning W, Sierkstra L, Neves MJ, Luyten K, Alijo R, Ramos J, Coccetti P. Molecular cloning of a gene involved in glucose sensing in the yeast *Saccharomyces cerevisiae*. *Mol Microbiol* 1993;8:927–43. [PubMed: 8355617]

36. Vuorio OE, Kalkkinen N, Londesborough J. Cloning of two related genes encoding the 56-kDa and 123-kDa subunits of trehalose synthase from the yeast *Saccharomyces cerevisiae*. *Eur J Biochem* 1993;216:849–61. [PubMed: 8404905]
37. Ausubel, FM.; Brent, R.; Kingston, RE.; Moore, DD.; Seidman, JG.; Smith, JA.; Struhl, K. *Current Protocols in Molecular Biology*. 1 - 3. Greene Publishing Associates, Inc. and John Wiley & Sons, Inc.; 2004.
38. Barham D, Trinder P. An improved colour reagent for the determination of blood glucose by the oxidase system. *Analyst* 1972;97:142. [PubMed: 5037807]
39. Trinder P. Determination of glucose in blood using glucose oxidase with an alternative oxygen acceptor. *Ann Clin Biochem* 1969;6:24.
40. Dahlqvist A. Assay of intestinal disaccharidases. *Anal Biochem* 1968;22:99–107. [PubMed: 5636962]
41. Bondar RJL, Mead DC. Evaluation of glucose-6-phosphate dehydrogenase from *Leuconostoc mesenteroides* in the hexokinase method for determining glucose in serum. *Clin Chem* 1974;20:586–590. [PubMed: 4363766]
42. Kunsst, A.; Draeger, B.; Ziegenhorn, J. *Methods of Enzymatic Analysis*. 2. Academic Press; New York: 1984.
43. Southgate, DAT. *Determination of Food Carbohydrates*. Applied Science Publishers; London: 1976.
44. Smith JD, Cappa CD, Wilson KR, Cohen RC, Geissler PL, Saykally RJ. Unified description of temperature-dependent hydrogen-bond rearrangements in liquid water. *Proc Nat Acad Sci* 2005;102:14171–14174. [PubMed: 16179387]
45. Nucci NV, Vanderkooi JM. Temperature dependence of hydrogen bonding and freezing behavior of water in reverse micelles. *J Phys Chem B* 2005;109:18301–18309. [PubMed: 16853355]
46. Wright WW, Guffanti G, Vanderkooi JM. Protein in sugar and glycerol/water as examined by IR spectroscopy and by the fluorescence and phosphorescence properties of tryptophan. *Biophys J* 2003;85:1980–95. [PubMed: 12944311]
47. Winkler A, Arkind C, Mattison CP, Burkholder A, Knoche K, Ota I. Heat stress activates the yeast high-osmolarity glycerol mitogen-activated protein kinase pathway, and protein tyrosine phosphatases are essential under heat stress. *Eukary Cell* 2002;1:163–173.
48. Efimov YY, Naberukhin YI. Fluctuation theory of hydrogen bonding applied to vibration spectra of HOD molecules in liquid water. I. Raman spectra. *Mol Phys* 2003;101:459–468.
49. Efimov YY, Naberukhin YI. Fluctuation theory of hydrogen bonding applied to vibration spectra of HOD molecules in liquid water. II. Infrared spectra: contour shape, integrated intensity, temperature dependence. *Mol Phys* 2004;102:1407–1414.
50. Sharp KA, Madan B, Manas E, Vanderkooi JM. Water structure changes induced by hydrophobic and polar solutes revealed by simulations and infrared spectroscopy. *J Chem Phys* 2001;114:1791–1796.
51. James TL, Gillen KT. Nuclear magnetic resonance relaxation time and self-diffusion constant of water in hen egg white and yolk. *Biochim Biophys Acta* 1972;286:10–15. [PubMed: 4676548]
52. Raaphorst GP, Kruuv J, Pintar MM. Nuclear magnetic resonance study of mammalian cell water: influence of water content and ionic environment. *Biophys J* 1975;15:391–402.

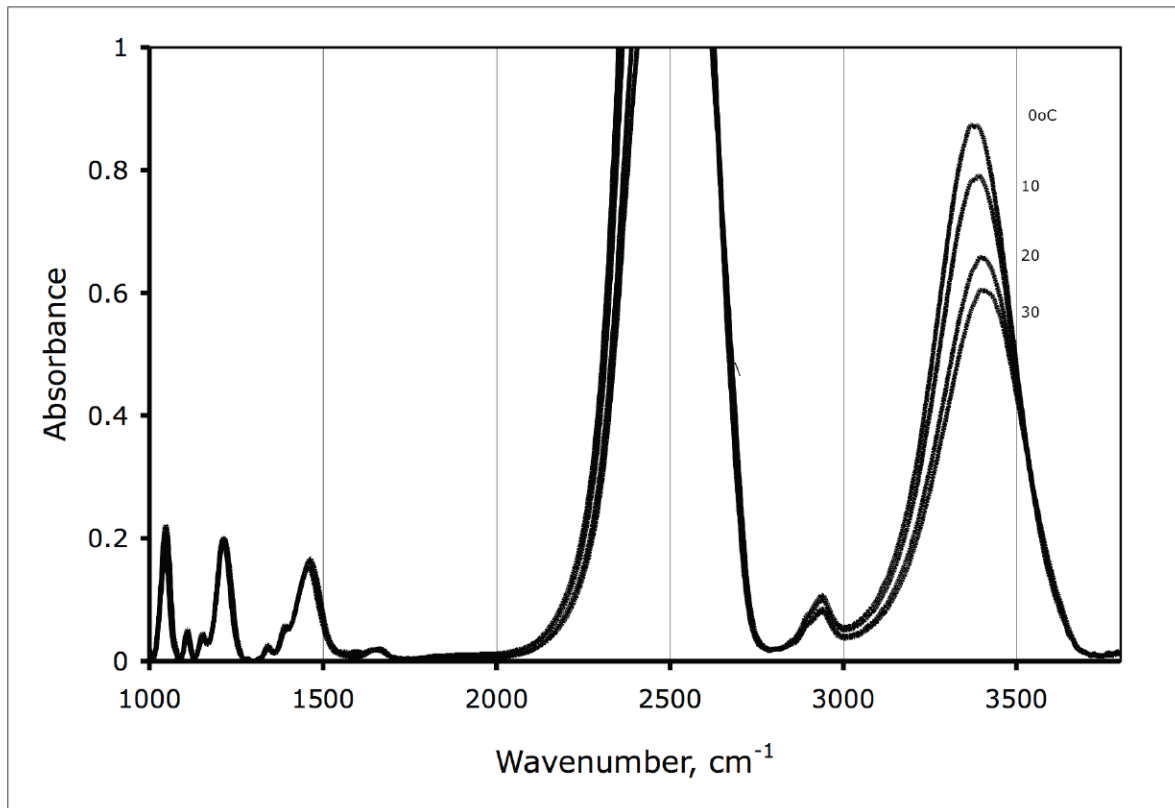


Figure 1. Infrared absorption spectrum of 1 M trehalose in 95 % D₂O and 5 % H₂O. The temperature is indicated on the Figure.

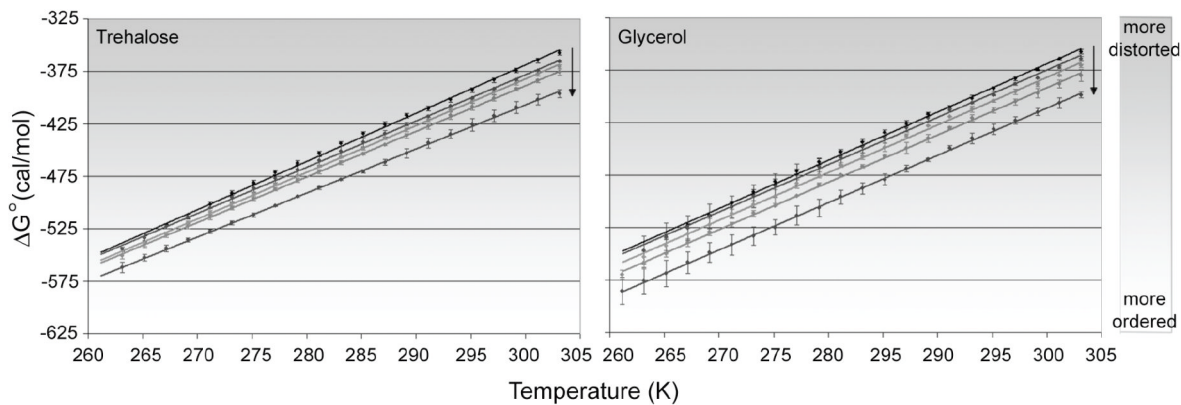


Figure 2.

Free energy analysis of the transition from high-energy to low-energy H-bonding for trehalose (left) and glycerol (right) at various concentrations. For trehalose, concentrations of 1 M, 500 mM, 250 mM, and 125 mM are shown. For glycerol, concentrations of 2 M, 1 M, 500 mM, and 250 mM are shown. In both graphs, water is represented by the black uppermost line. Arrows indicate direction of increasing concentration. All solutions are approximately 80% deuterated at exchangeable hydrogen sites. Measurements were performed in duplicate for each condition. Error bars represent one standard deviation.

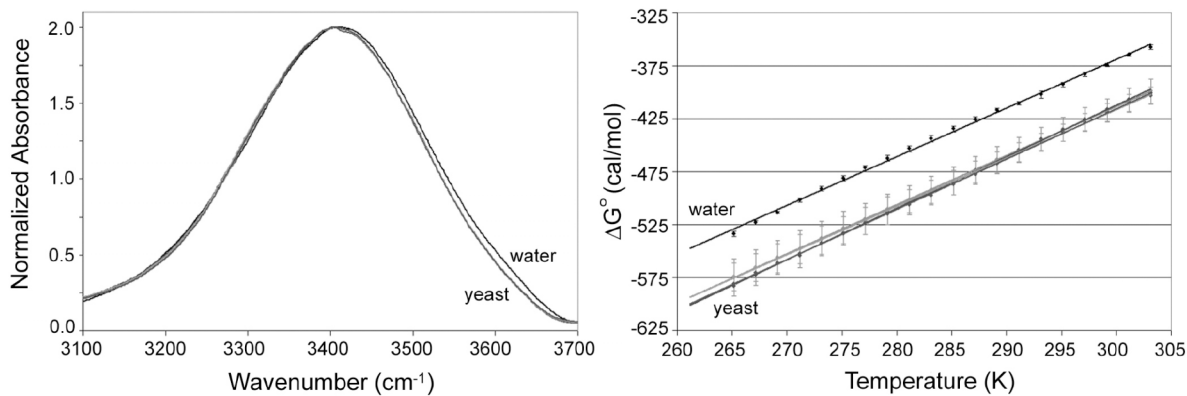


Figure 3.

Normalized OH stretch spectra (left) at 303 K for water, constitutive YHN429 and YHN432, and heat-shocked YHN429 and YHN432. Note that the yeast plots cannot be differentiated and are labeled collectively as “yeast” on the graphs. Free energy analysis of the transition from high-energy to low-energy H-bonding as a function of temperature for the same conditions is shown on the right. Water controls were approximately 80% deuterated at exchangeable hydrogen sites while yeast samples had higher deuterium content (greater than 90%). Measurements were performed in duplicate for water and triplicate for the constitutive Y429 and Y432 strains. Error bars represent one standard deviation.

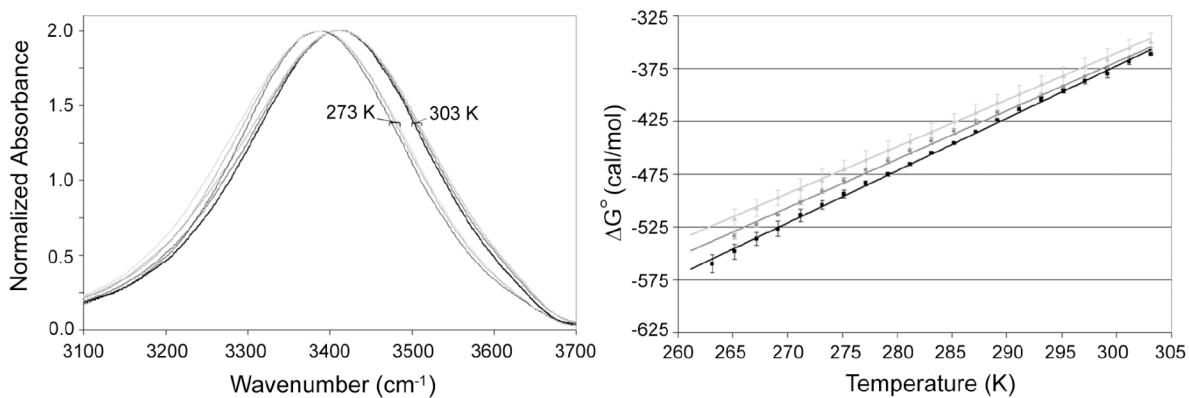


Figure 4. Normalized OH stretch spectra (left) at 303 K (heavy lines) and 273 K (thin lines) for 90% D₂O/10% H₂O (v/v) (black), 80% D₂O/20% H₂O (v/v) (gray), 70% D₂O/30% H₂O (v/v) (light gray). Free energy analysis of the transition from high-energy to low-energy H-bonding as a function of temperature for the same conditions is shown on the right. Measurements were performed in duplicate for all conditions. Error bars represent one standard deviation.

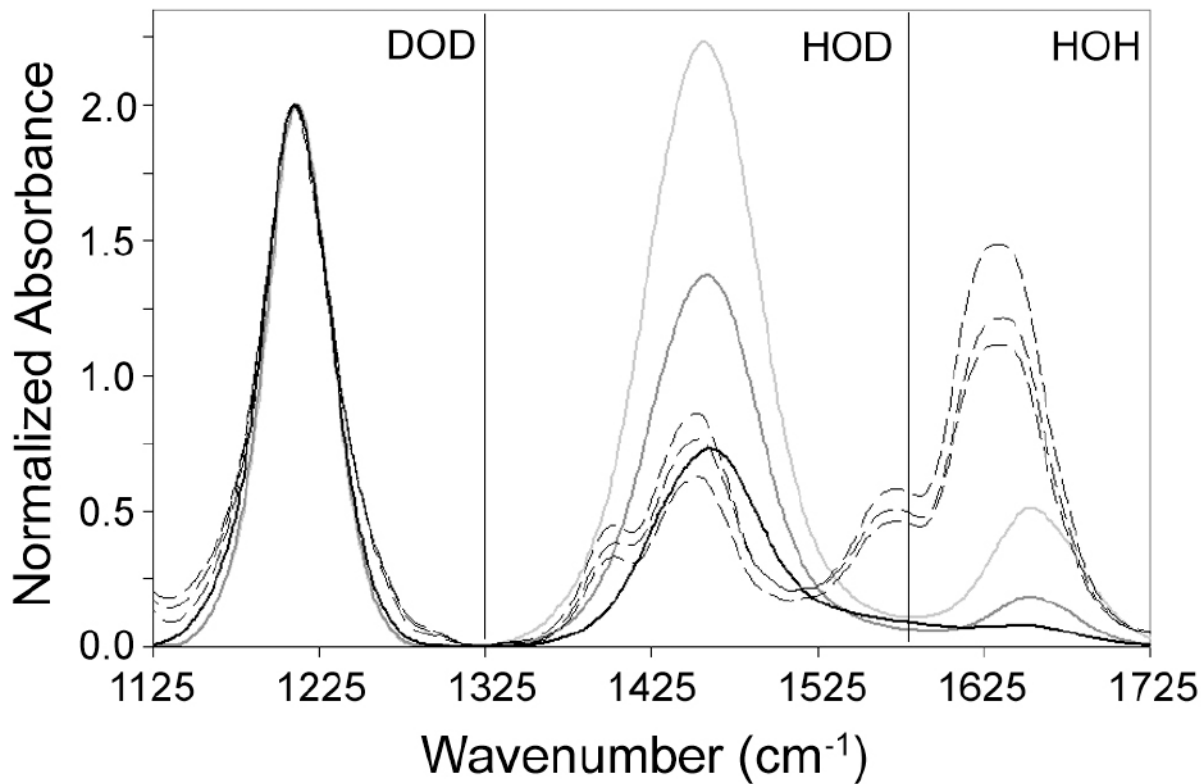


Figure 5. Normalized DOD bend spectra at 303 K for 90% D₂O/10% H₂O (v/v) (heavy black), 80% D₂O/20% H₂O (v/v) (heavy gray), 70% D₂O/30% H₂O (v/v) (heavy light gray) and constitutive YHN432 yeast replicates (dashed black lines). The spectra are extended to include the HOD and HOH bend regions for estimation of deuterium content in samples.